Tilted Fiber Bragg Grating for Chirped Microwave Waveform Generation

Ming Li, *Member, IEEE*, Li-Yang Shao, Jacques Albert, *Member, IEEE*, and Jianping Yao, *Senior Member, IEEE*

***Abstract*—A tilted fiber Bragg grating (TFBG) as an optical spectral shaper to generate a chirped microwave waveform in a spectral-shaping and wavelength-to-time (SS-WTT) mapping system is proposed and demonstrated. The key component in the system is the TFBG, which has multiple resonant peaks with linearly increasing spacing in its transmission spectrum. By incorporating a TFBG into an SS-WTT system, a chirped microwave waveform is generated with the chirp rate determined by the tilt angle of the TFBG. A proof-of-concept experiment is carried out. Two TFBGs with tilt angles of 10° and 4° are fabricated and employed to generate two chirped microwave waveforms with chirp rates of 0.00700 and 0.05956 GHz/ps, respectively.**

***Index Terms*—Chirped microwave waveform generation, tilted fiber Bragg gratings (TFBGs), wavelength-to-time mapping.**

I. Introduction

PHOTONIC generation of chirped microwave waveforms has been a topic of interest recently. Chirped microwave waveforms can find many important applications such as modern radar, ultrafast wired and wireless communications, medical imaging and modern instrumentation [1]. The key advantages of using photonic techniques for chirped microwave waveform generation are the ultrafast speed and broad bandwidth, which cannot be realized using currently available electronic techniques. Numerous photonically assisted techniques have been proposed recently to generate chirped microwave waveforms [2]–[5]. Among them, chirped microwave waveform generation based on pure fiber optics offers advantages such as smaller size, lower loss, better stability and higher potential for integration.

Optical spectral-shaping and wavelength-to-time (SS-WTT) mapping is an important technique which has been recently employed to generate chirped microwave waveforms [4], [5]. In an SS-WTT mapping system, chirped microwave waveform generation is implemented by shaping the spectrum of an ultrashort optical pulse with a spectral filter that has a increasing or decreasing free spectral range (FSR) and then the spectrum-shaped pulse is linearly mapped to the time domain in a dispersive element [4]. Due to the linear wavelength-to-time mapping, a chirped microwave waveform with a shape that is a scaled version of the shaped spectrum is generated [4]. The key device in an SS-WTT system for a chirped microwave waveform generation is the spectral filter, which should have a spectrum with increasing or decreasing FSR. Such a spectral filter can be achieved using superimposed FBGs [6] or a Sagnac-loop mirror incorporating a chirped fiber Bragg grating [7].

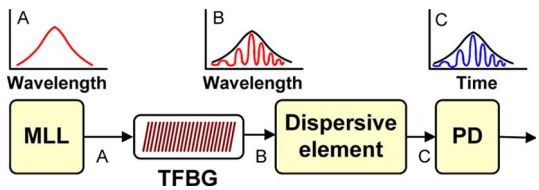

Fig. 1. Schematic of the chirped microwave waveform generator using a TFBG. PD: Photodetector. MLL: Mode-locked laser. TFBG: tilted fiber Bragg grating.

In this letter, we proposed to generate a chirped microwave waveform based on SS-WTT mapping using a tilted fiber Bragg grating (TFBG) as the optical spectral filter. The key feature of the TFBG is that there are multiple cladding-mode resonant peaks with approximately increasing or decreasing spacing in its transmission spectrum. Compared to other types of resonant filters with varying FSR [6], [7], the TFBG has several advantages such as ease of fabrication, very small insertion loss, wide bandwidth and relatively little temperature sensitivity [8]. In addition, there is some flexibility in shaping the amplitude envelope of the resonant peaks by varying the tilt angle. Two TFBGs with tilt angles of 10° and 4° are fabricated and employed to generate two chirped microwave waveforms with two chirp rates of 0.00700 and 0.05956 GHz/ps, respectively.

II. Principle and System Configuration

The schematic of the proposed chirped microwave waveform generator using a TFBG is shown in Fig. 1. A transform-limited ultrashort optical pulse from a mode locked laser (MLL) is sent to the TFBG that is working in the transmission mode. The TFBG is used to shape the power spectrum of the input optical pulse to have a spectrum that has linearly increasing wavelength spacing for the cladding mode resonant wavelengths. After the TFBG, a dispersive element with a linear group delay response is used to perform the dispersion-induced wavelength-to-time mapping. A microwave waveform with its shape that is a scaled version of the shaped optical power spectrum is then generated at the output of a photodetector (PD).

Manuscript received July 28, 2010; revised November 17, 2010; accepted December 18, 2010. Date of publication December 23, 2010; date of current version February 24, 2011. This work was supported by the Natural Sciences and Engineering Research Council of Canada (NSERC).

M. Li and J. Yao are with the Microwave Photonics Research Laboratory, School of Information Technology and Engineering, University of Ottawa, Ottawa, ON K1N 6N5, Canada (e-mail: mingli02@site.uOttawa.ca; jpyao@site.uOttawa.ca).

L.-Y. Shao and J. Albert are with the Department of Electronics, Carleton University, Ottawa, ON K1S 5B6, Canada (e-mail: liyangshao@gmail.com; jalbert@doe.carleton.ca).

Color versions of one or more of the figures in this letter are available online at http://ieeexplore.ieee.org.

Digital Object Identifier 10.1109/LPT.2010.2102013

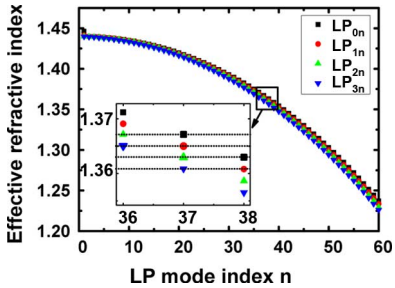

Fig. 2. Effective refractive indices of the LP modes of a TFBG. A zoom-in view of the indices is shown in the inset.

The key component in the system is the TFBG. It is different from a regular FBG, a TFBG has a transmission spectrum with the longest wavelength resonance corresponding to the reflection of the core mode and the shorter wavelength resonances corresponding to the contra-propagating coupling between the core mode and the cladding modes. The resonant wavelength in transmission is given by

$$\lambda_{\mathrm{clad},i} = \left(n_{\mathrm{eff,clad},i} + n_{\mathrm{eff,core}}\right) \frac{\Lambda_g}{\cos\theta}, \tag{1}$$

where $n_{\mathrm{eff,core}}$ and $n_{\mathrm{eff,clad},i}$ are the effective refractive indices of the core mode and the ith cladding mode, respectively, Λ_g is the nominal grating period and θ is the tilt angle. Since $n_{\mathrm{eff,core}}$ is almost kept constant within the related wavelength band, the wavelength spacing is given by

$$\Delta\lambda_{\mathrm{clad},i,i+1} = \left(n_{\mathrm{eff,clad},i+1} - n_{\mathrm{eff,clad},i}\right) \frac{\Lambda_g}{\cos\theta}. \tag{2}$$

As can be seen from (2), the relationship between the wavelength spacing and the wavelength is determined by the effective refractive index of cladding modes. The effective refractive index of the linear polarization (LP) modes are calculated and shown in Fig. 2. Since the coupling coefficient of the LP_{mn} $(m \geq 4)$ mode in a TFBG is very small and can be neglected, only the effective refractive indexes of the LP_{mn} $(m \leq 3)$ modes are considered [9]. The transmission spectrum of a TFBG is formed based on the coupling between the four series of the LP modes and the core mode. Fig. 2 shows that each notch response is determined by two LP modes which have almost the same effective refractive index. Therefore, the wavelength spacing can be approximately calculated based on the half value of the effective refractive index difference between two neighboring LP modes (e.g., $\mathrm{LP}_{0,36}$ and $\mathrm{LP}_{0,37}$ which are approximately half separated by $\mathrm{LP}_{1,36}$).

Fig. 3 shows the simulated relationship between the wavelength spacing and the wavelength. In the simulation, the tilt angle of the TFBG is 10° and the Bragg wavelength is 1600 nm. The wavelength spacing is not linearly decreasing within the whole wavelength band. However, it is linearly decreasing within a small wavelength range. As shown in the inset of Fig. 3, the wavelength spacing is linearly decreasing from 1550 nm to 1570 nm which covers the bandwidth of the MLL used for the experiment). Since we have the mapping relation between the time and wavelength $t = \lambda \times \ddot{\Phi}$, the instantaneous frequency f is given by $f = 1/\Delta t = 1/(\ddot{\Phi} \times \Delta\lambda)$, where Δt is the time spacing, $\ddot{\Phi}$ is the chromatic dispersion (ps/nm) and

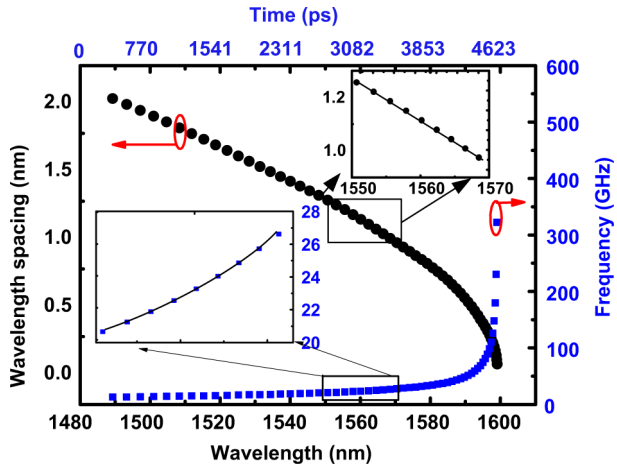

Fig. 3. Wavelength spacing versus wavelength and the simulated instantaneous frequency versus time. The insets show the zoom-in views of the two curves.

$\Delta\lambda$ is the wavelength spacing. The dispersive element in the simulation has a value of chromatic dispersion of 38.53 ps/nm. The instantaneous frequency is calculated and shown in Fig. 3. As can be seen from the zoom-in view, the instantaneous frequency mapped from the wavelength domain from 1550 to 1570 nm is approximately linear. Thus, an approximately linearly chirped microwave waveform is generated using a TFBG in an SS-WTT mapping system.

III. Experiment

An experiment based on the setup shown in Fig. 1 is then carried out. An ultrashort pulse with a pulse-width of 550 fs, a full-width at half-maximum (FWHM) bandwidth of 8 nm and a central wavelength of 1558.6 nm generated by the MLL is sent to the TFBG.

First, a TFBG with a tilt angle of 10° is employed. The transmission spectrum of the TFBG is shown in Fig. 4(a). The Bragg wavelength is about 1603.1 nm. The fabrication of a TFBG was described in [10]. Fig. 4(a) shows that the wavelength spacing between two neighboring resonant wavelengths is almost linearly decreasing with the increase of wavelength with a decreasing slope of -0.01005 nm/nm. In addition, as can be seen from the inset of Fig. 4(a), the wavelength resonance is formed by two closely spaced notch responses due to the coupling between the LP modes with core mode. The experimental results confirm the theoretical analysis in Section II. The TFBG is then used to shape the power spectrum of the input optical pulse. The wavelength spacing at the central wavelength of the shaped power spectrum is 1.09 nm. The spectrum-shaped optical pulse is then directed into a 2.3 km single mode fiber (SMF) with a chromatic dispersion value of 38.53 ps/nm. After the dispersion-induced linear frequency-to-time mapping in the SMF, the spectrum-shaped power spectrum is mapped to the time domain. A chirped microwave waveform is thus experimentally generated, as shown in Fig. 4(b). The instantaneous frequency within the main waveform lobe is also shown in Fig. 4(b). As can be seen the instantaneous frequency is increasing approximately linearly with time with a central frequency of 24.21 GHz and a chirp rate of 0.00700 GHz/ps. Based on (1), the theoretically

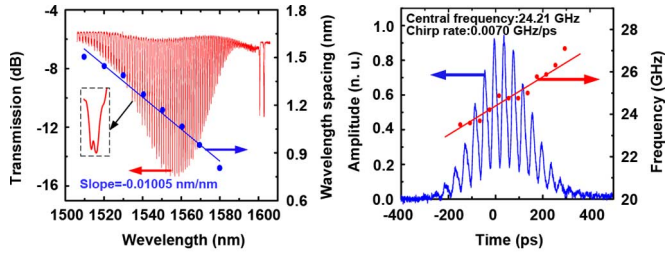

(a) (b)

Fig. 4. (a) Transmission spectrum of the TFBG with a 4° tilt angle used in the experiment. The dotted line shows the wavelength spacing between two neighboring resonant wavelengths as a function of optical wavelength. (b) Experimental result: the generated linearly chirped microwave waveform (solid blue line) and the instantaneous frequency (red dots). Solid red line is the linear fitting of the instantaneous frequency.

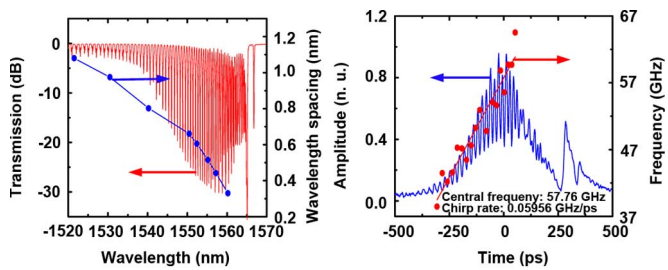

(a) (b)

Fig. 5. (a) Transmission spectrum of the TFBG with a 4° tilt angle used in the experiment. The dotted line shows the wavelength spacing between two neighboring resonant wavelengths as a function of optical wavelength. (b) Experimental result: the generated linearly chirped microwave waveform (solid blue line) and the instantaneous frequency (red dots). Solid red line is the linear fitting of the instantaneous frequency.

calculated central frequency is 23.80 GHz and the chirp rate is 0.0062 GHz/ps. An excellent agreement is reached.

Then, in the second experiment, a TFBG with a different tilt angle of 4° is incorporated into the system. The transmission spectrum of the 4° TFBG is shown in Fig. 5(a). The wavelength spacing at the central wavelength of the shaped power spectrum is 0.442 nm. The Bragg wavelength is about 1567.0 nm that is close to the central wavelength of the MLL. Similar to the theoretical results in Fig. 3, the measured wavelength spacing between two neighboring resonant wavelengths is rapidly decreasing when the wavelength gets close to the Bragg wavelength. Fig. 5(b) shows the measured microwave waveform. The central frequency is 57.76 GHz and the chirp rate is 0.05956 GHz/ps. The chirp rate of the generated microwave waveform in the second experiment is about 8.5 times higher than that in the first experiment using the 10° TFBG.

IV. Discussion

As shown in Fig. 5, since the Bragg wavelength of the TFBG falls in the spectral range of the MLL, the right part of the generated chirped microwave waveform is not as good as the left part. A phase mask with a larger period may be used to shift the Bragg wavelength out of the spectral range of the MLL. In addition, once a TFBG is fabricated, its transmission spectrum is hard to be largely tuned. Therefore, it is difficult to change the chirp rate of the generated microwave waveform by tuning the TFBG mechanically or thermally. However, as can be seen from Fig. 3, the wavelength spacing along the wavelength is continuously decreasing, it is possible to tune the chirp rate of the generated chirped microwave waveform at a high speed by tuning the wavelength of a wavelength-tunable MLL [11].

The temporal duration of the two generated chirped microwave waveforms is about 300 ps. The pulse width can be increased by increasing the bandwidth of the MLL or increasing the dispersion value of the dispersive element. As shown in Fig. 3, when the spectral width of the MLL is largely increased, the generated chirped microwave waveform will not be linearly chirped. There exists a trade-off between the pulse duration and the linearity of the generated chirped microwave waveform. On the other hand, increasing the dispersion value of the dispersive element will result in an increase in the pulse duration, but the central frequency will decrease accordingly.

V. Conclusion

A novel approach to generating a linearly chirped microwave waveform based on SS-WTT mapping using a TFBG as a spectral filter was proposed and experimentally demonstrated. The key component in the proposed system was the TFBG. Since a TFBG has a transmission spectrum with linearly increasing wavelength spacing for the cladding mode resonant wavelengths, the incorporation of the TFBG into a SS-WTT mapping system can generate a linearly chirped microwave waveform. In the experiment, two TFBGs with tilt angles of 10° and 4° were fabricated and employed to generate two chirped microwave waveforms with chirp rates of 0.00700 and 0.05956 GHz/ps, respectively.

References

[1] A. M. Weiner, "Femtosecond pulse shaping using spatial light modulators," *Rev. Sci. Instrum.*, vol. 71, no. 5, pp. 1929–1960, May 2000.

[2] J. Chou, Y. Han, and B. Jalali, "Adaptive RF-photonic arbitrary waveform generator," *IEEE Photon. Technol. Lett.*, vol. 15, no. 4, pp. 581–583, Apr. 2003.

[3] J. D. McKinney, D. E. Leaird, and A. M. Weiner, "Millimeter-wave arbitrary waveform generation with a direct space-to-time pulse shaper," *Opt. Lett.*, vol. 27, no. 15, pp. 1345–1347, Aug. 2002.

[4] H. Chi and J. P. Yao, "All-fiber chirped microwave pulses generation based on spectral shaping and wavelength-to-time conversion," *IEEE Trans. Microw. Theory Tech.*, vol. 55, no. 9, pp. 1958–1963, Sep. 2007.

[5] C. Wang and J. P. Yao, "Photonic generation of chirped millimeter-wave pulses based on nonlinear frequency-to-time mapping in a nonlinearly chirped fiber Bragg grating," *IEEE Trans. Microw. Theory Tech.*, vol. 56, no. 2, pp. 542–553, Feb. 2008.

[6] C. Wang and J. P. Yao, "Photonic generation of chirped microwave pulses using superimposed chirped fiber Bragg gratings," *IEEE Photon. Technol. Lett.*, vol. 20, no. 11, pp. 882–884, Jun. 1, 2008.

[7] C. Wang and J. P. Yao, "Chirped microwave pulse generation based on optical spectral shaping and wavelength-to-time mapping using a sagnac-loop mirror incorporating a chirped fiber Bragg grating," *J. Lightw. Technol.*, vol. 27, no. 16, pp. 3336–3341, Aug. 15, 2009.

[8] T. Guo, A. Ivanov, C. Chen, and J. Albert, "Temperature-independent tilted fiber grating vibration sensor based on cladding-core recoupling," *Opt. Lett.*, vol. 33, no. 9, pp. 1004–1006, May 2008.

[9] K. S. Lee and T. Erdogan, "Fiber mode coupling in transmissive and reflective fiber gratings," *Appl. Opt.*, vol. 39, no. 9, pp. 1394–1404, Mar. 2000.

[10] C. Chan, C. Chen, A. Jafari, A. Laronche, D. J. Thomson, and J. Albert, "Optical fiber refractometer using narrowband cladding-mode resonance shifts," *Appl. Opt.*, vol. 46, no. 7, pp. 1142–1149, Mar. 2007.

[11] H. Sotobayashi, J. T. Gopinath, E. M. Koontz, L. A. Kolodziejski, and E. P. Ippen, "Wavelength tunable passively mode-locked bismuth oxide-based erbium-doped fiber laser," *Opt. Commun.*, vol. 237, no. 4–6, pp. 399–403, Jul. 2004.